

Dynamic Mix Precision Routing for Efficient Multi-step LLM Interaction

Yuanzhe Li¹ Jianing Deng² Jingtong Hu² Tianlong Chen³ Song Wang⁴ Huanrui Yang¹

Abstract

Large language models (LLM) achieve strong performance in long-horizon decision-making tasks through multi-step interaction and reasoning at test time. While practitioners commonly believe a higher task success rate necessitates the use of a larger and stronger LLM model, multi-step interaction with a large LLM incurs prohibitive inference cost. To address this problem, we explore the use of low-precision quantized LLM in the long-horizon decision-making process. Based on the observation of diverse sensitivities among interaction steps, we propose a dynamic mix-precision routing framework that adaptively selects between high-precision and low-precision LLMs at each decision step. The router is trained via a two-stage pipeline, consisting of KL-divergence-based supervised learning that identifies precision-sensitive steps, followed by Group-Relative Policy Optimization (GRPO) to further improve task success rates. Experiments on ALFWorld demonstrate that our approach achieves a great improvement on accuracy–cost trade-off over single-precision baselines and heuristic routing methods.

1. Introduction

Large language models have demonstrated strong performance across a wide range of tasks, including complex agentic settings that require long-horizon decision making, tool use, and interaction with environments (Yao et al., 2022b; Schick et al., 2023; Wang et al., 2024a; Shinn et al., 2023; Yang et al., 2024). However, deploying LLM on such complex tasks incurs substantial computational costs (Wang et al., 2025; Si et al., 2025).

Quantization shows up as a promising method to improve the efficiency of LLM at test time. Recent work has shown that post-training quantization effectively preserves perfor-

¹University of Arizona ²University of Pittsburgh ³University of North Carolina at Chapel Hill ⁴University of Central Florida. Correspondence to: Huanrui Yang <huanruiyang@arizona.edu>.

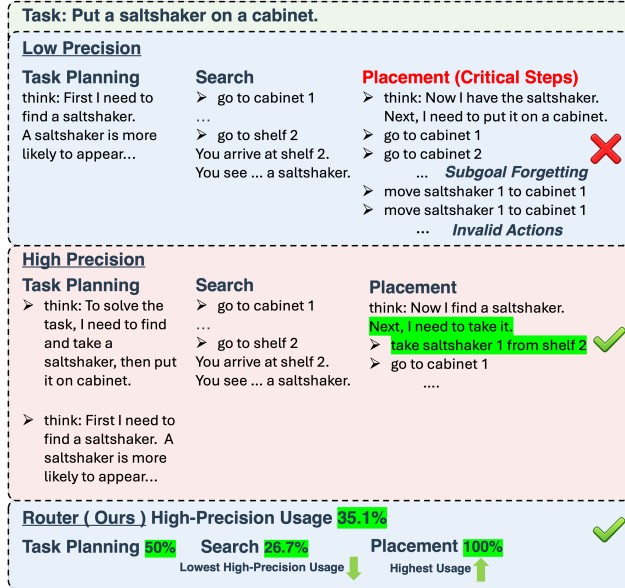


Figure 1. Reasoning Case Study. Compared to the high precision model, the low precision model failed at certain critical steps. Our router successfully judges the difficulty of each step and provide an efficient combination of model executions that succeeds the task with a fraction of high precision model usage.

mance on many static benchmarks (Dettmers et al., 2022; Lin et al., 2024). However, LLM quantization leads to significant degradation on real-world agentic tasks that involve structured workflows, tool use, and long-context understanding (Dong et al., 2025; Jin et al., 2024). This observation suggests that naively applying quantization throughout an agent’s execution may be fundamentally mismatched with the requirements of agentic interaction.

To balance the performance and efficiency, we tackle the challenge by observing the failed reasoning trajectories of quantized LLMs. We observe a step-wise diversity in sensitivity against model quantization: While the quantized model works well in earlier reasoning steps, it will likely encounter some “*critical steps*” that is out of its capability, which leads to wrong reasoning outcome in the end as illustrated in Figure 1, the placement phase is one such critical step. Based on this observation, we propose to combine the complementary strengths of full-precision and quantized models by introducing a router that dynamically selects between models (Ong et al., 2025a;b; Ding et al.,

2025; Yue et al., 2025; Jitkrittum et al., 2025). However, existing routing methods are primarily designed for static or simplified settings, such as general QA, or mathematical reasoning, and operate at the question level, which is too coarse-grained for real-world, long-horizon agentic tasks.

Motivated by these limitations, we propose a lightweight dynamic router that operates at the step level. Our method adaptively selects between full-precision and quantized models at each decision step, enabling efficient computation while preserving the robustness required for real-world agentic tasks. This step-level routing provides a principled middle ground between coarse question-level routing and overly fine-grained token-level coordination, effectively integrating the advantages of both high- and low-precision models.

Taken together, this work revisits precision selection from a sequential decision-making perspective and demonstrates that dynamic, step-level precision control is effective in agentic setting. Building on this insight, we make the following contributions.

- We introduce a **dynamic mix-precision framework** for long-horizon agentic tasks. Our method substantially reduces inference cost while maintaining task success rates in the challenging interactive environment.
- We further optimize the mix-precision policy using **reinforcement learning**, enabling the agent to jointly balance task performance and inference cost.
- We demonstrate that effective precision routing does not require a full-capacity language model. A **lightweight router** of two-layers Transformer Encoder is sufficient to identify precision-critical steps.

2. Related Work

LLM Agentic Tasks. Recent work has increasingly focused on applying large language models to agentic settings that require long-horizon decision making (Yao et al., 2022b; Qiao et al., 2025; Li et al., 2025a), tool use (Schick et al., 2023; Wu et al., 2024), and interaction with environments (Wang et al., 2024a; Yang et al., 2024; Wang et al., 2024b). These agentic tasks arise in multiple forms, including text-based embodied environments such as ALF-World (Shridhar et al., 2021) and ScienceWorld (Wang et al., 2022), as well as representative benchmarks for tool use (Wang et al., 2024b), web navigation (Zhou et al., 2024; Yao et al., 2022a) and software engineering (Jimenez et al., 2024). Despite differences in surface form, these settings share a common structure of sequential, state-dependent decision making: each step involves observing the current state, selecting an action, and receiving new observations. In this work, we focus on embodied, environment-based

benchmarks as a representative subclass of this broader agentic paradigm, as they exhibit the same common structure of sequential, state-dependent decision making over long horizons in multi-step interactions.

LLM Routing. Routing mechanisms have been widely studied as a way to combine the complementary strengths of multiple language models while optimizing the performance–cost trade-off. Early approaches typically make a single routing decision at the query level and are primarily evaluated on single-turn benchmarks.

FrugalGPT (Chen et al., 2024a) pioneers a cascading framework that sequentially invokes models from cheap to expensive. In parallel, ensemble-based approaches such as LLM-Blender (Jiang et al., 2023) aggregate outputs from multiple candidate models via pairwise ranking and generative fusion.

Other works adopt learned discriminative routers. HybridLLM (Ding et al., 2024) predicts query difficulty to route inputs between models under quality constraints, while RouterDC (Chen et al., 2024b) aligns query and model representations through dual contrastive learning. Building on these ideas, RouteLLM (Ong et al., 2025b) learns efficient routing policies from human preference data, and BEST-Route (Ding et al., 2025) further incorporates test-time compute allocation. At a finer granularity, recent work explores token-level fusion and routing across multiple experts models (Xiong et al., 2026).

Beyond single-turn routing, (Zhang et al., 2025) (Router-R1) formulates routing as a sequential decision process, allowing routing decisions to be made dynamically across multiple reasoning steps. Nevertheless, their task setting remains limited to static Question Answering (QA).

Relatedly, Mixture-of-Experts (MoE) models (Shazeer et al., 2017) employ conditional routing to activate sparse expert parameters within a single model. In contrast, MoE methods introduce additional expert parameters, whereas our approach only leverages quantized variants derived from the same base model.

Quantization in LLM Agent. While traditional quantization benchmarks primarily focus on static language modeling metrics such as perplexity, recent work has started to examine the effects of compression in dynamic, agentic settings. (Dong et al., 2025; Li et al., 2025b) shows that 4-bit quantization leads to a substantial accuracy drop when deployed in real-world interactive environments and degrades numerical computation and reasoning ability. (Liu et al., 2025) conduct a comprehensive study of reasoning models and demonstrate that task difficulty has a significant impact on their performance.

3. Problem Formulation

We study a dynamic precision routing problem in multi-step agentic tasks. Let $\mathcal{M} = \{M^{(1)}, \dots, M^{(K)}\}$ denote a set of language models derived from the same base model under different numerical precisions. Each $M^{(k)}$ induces a policy $\pi^{(k)}(a \mid s)$ over a shared action space \mathcal{A} and incurs an inference cost $c^{(k)}$.

At each step t , the agent receives a textual observation s_t from a partially observable environment. The observation s_t consists of the task description, current environment description, and a history of past actions and observations.

To dynamically select which language model to use at each step, we introduce a routing policy

$$r_t = R_\theta(s_t), \quad r_t \in \{1, \dots, K\}, \quad (1)$$

parameterized by θ , which maps the current observation to a model index. Based on s_t and the routing decision r_t , the agent samples an action $a_t \sim \pi^{(r_t)}(\cdot \mid s_t)$, which is executed to produce the next observation s_{t+1} .

An episode terminates when a task-specific success condition is satisfied or the maximum step limit T is reached. The agent receives a task-level reward $R(\tau)$, which is typically sparse and only provided at the end of the episode, where $\tau = \{(s_t, a_t)\}_{t=1}^T$ and the terminal reward $r_T = R(\tau)$ denotes a trajectory.

Our objective is to maximize the expected task reward while minimizing the cumulative inference cost:

$$\max_{\theta} \mathbb{E}_{\tau \sim p_{\theta}} \left[R(\tau) - \lambda \sum_{t=1}^{|\tau|} c^{(r_t)} \right], \quad (2)$$

where $\lambda \geq 0$ controls the trade-off between performance and efficiency. Unlike prior approaches that route at the query or episode level, this formulation enables fine-grained, step-level model selection within long-horizon decision-making tasks.

4. Method

We propose a two-stage training framework for step-level mix-precision routing, consisting of (i) KL-divergence-based supervised training (KL-ST), and (ii) Group-Relative Policy Optimization (GRPO). An overview of the proposed framework is illustrated in Figure 2.

4.1. Router Architecture

We design a lightweight router that performs *step-level precision selection* based on the agent’s interaction trajectory history. The router is explicitly decoupled from action generation and environment interaction with LLM, and is invoked

solely to decide which numerical precision to apply at each decision step.

Step-Level State Representation. At decision step t , the agent’s state is represented as a sequence of step-level embeddings

$$X_t = [z_1, z_2, \dots, z_t], \quad z_i \in \mathbb{R}^d, \quad (3)$$

where each token z_i is a compact embedding summarizing the agent’s interaction at step i , including the environment observation and action at time step i . The embeddings are pre-computed by an external encoder and treated as fixed inputs to the router. To handle variable-length trajectories, we associate a binary mask

$$m_t \in \{0, 1\}^t, \quad (4)$$

indicating valid tokens, and optionally truncate the sequence to a maximum length L_{\max} for efficiency.

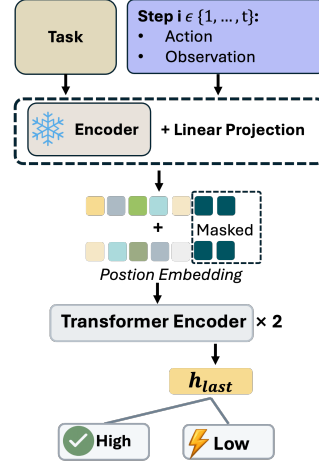


Figure 3. Step-level routing architecture with masked position-aware representations. The task description and each trajectory step (action–observation pair) are encoded by a frozen text encoder, producing a sequence of step embeddings. Learnable position embeddings are added to inject step-order information, while a binary mask is applied to ignore invalid or truncated steps in variable-length trajectories. A transformer encoder processes the masked sequence, and the hidden state of the last valid step is used to predict.

Router Network. The router is parameterized as a lightweight Transformer encoder with $N = 2$ layers. Given the input sequence X_t , we first add learned absolute positional embeddings:

$$\tilde{X}_t = X_t + P_t, \quad (5)$$

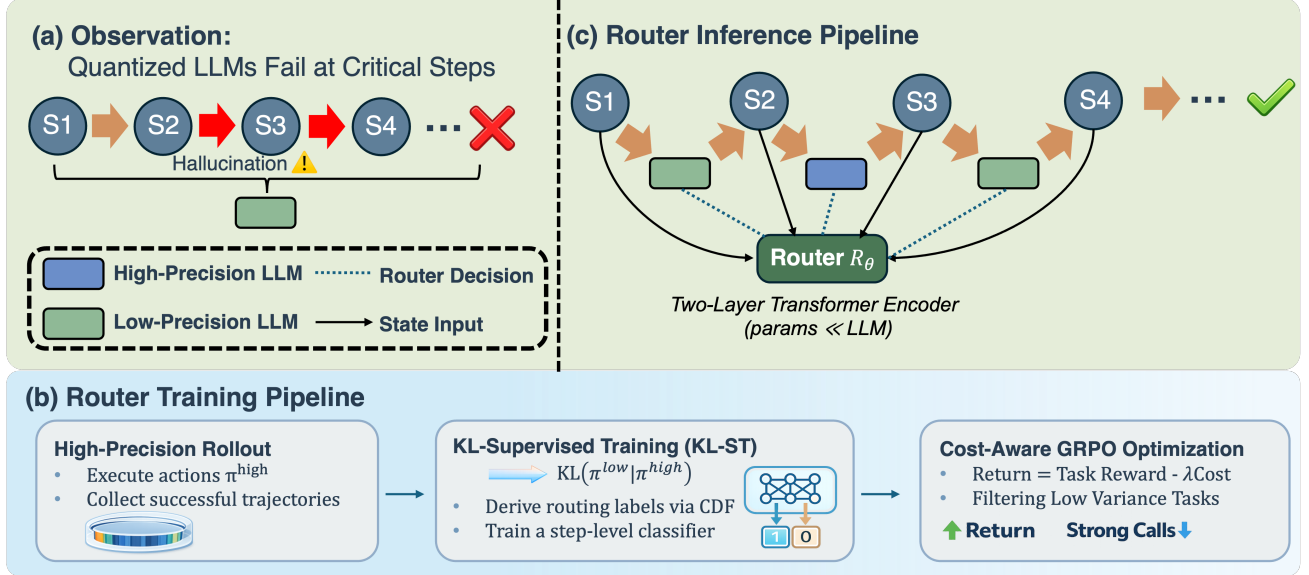


Figure 2. Overview of our dynamic mix-precision routing framework. (a) *Observation*: From the failed reasoning trajectories of quantized LLMs, we observe a step-wise diversity in sensitivity against model quantization: The quantized model will likely to encounter some “critical steps” that is out of its capability, which leads to wrong reasoning outcome in the end. (b) *Router training pipeline*: We collect high-precision successful rollouts and derive binary supervision signals from KL divergence to train a lightweight two-layers Transformer router that predicts whether a step is precision-sensitive. The router is further refined using group-relative policy optimization (GRPO) with a cost-aware reward to balance task success and inference efficiency. (c) At inference time, the router dynamically selects between a high-precision LLM and a quantized LLM at each decision step.

where $P_t \in \mathbb{R}^{t \times d}$ denotes the positional embedding matrix. The encoded hidden states are computed as

$$H_t = \text{TransformerEnc}_\theta(\tilde{X}_t, m_t), \quad (6)$$

where $H_t = [h_1, h_2, \dots, h_t]$ and the attention mask ensures that padded positions do not contribute to the computation.

Pooling and Routing Decision. To obtain a step-level routing decision, we apply *last-token pooling* and extract the hidden state corresponding to the most recent valid step:

$$h_t^* = h_{\sum_{i=1}^t m_t(i)}. \quad (7)$$

The router then outputs a categorical distribution over available precision levels:

$$\pi_\theta(r_t | s_t) = \text{Softmax}(W h_t^*), \quad r_t \in \{1, \dots, K\}, \quad (8)$$

where each r_t corresponds to invoking a language model instantiated at a specific numerical precision (e.g., bf16 or int4 / 3bit).

During training, routing decisions are sampled from π_θ to encourage exploration, while at inference time the router may act greedily. The architecture of the router is depicted in Figure 3.

4.2. KL-ST Stage

Our KL-based supervision is motivated by an empirical observation: although low-precision models often perform comparably to high-precision models across most decision steps, they occasionally exhibit severe behavioral divergence at a small subset of steps, which frequently leads to catastrophic and irreversible trajectory-level failures. Empirically, we find that these failures are concentrated at a small number of critical decision points rather than being uniformly distributed along the trajectory (Figure 4).

To characterize this phenomenon, we measure the step-wise KL divergence between the action distributions of low-precision and high-precision models. The resulting KL divergence distribution is highly skewed, with most steps exhibiting small divergence values and a heavy tail corresponding to rare but significant deviations. These high-divergence steps align closely with critical decisions where low-precision models deviate substantially from high-precision behavior.

Trajectory Sampling Protocol. To obtain reliable KL supervision, we collect data using a high-precision rollout strategy. At each decision step t , we compute action distributions from both the low-precision model $\pi^{\text{low}}(\cdot | s_t)$ and the high-precision reference model $\pi^{\text{high}}(\cdot | s_t)$, but always execute the action sampled from π^{high} in the environ-

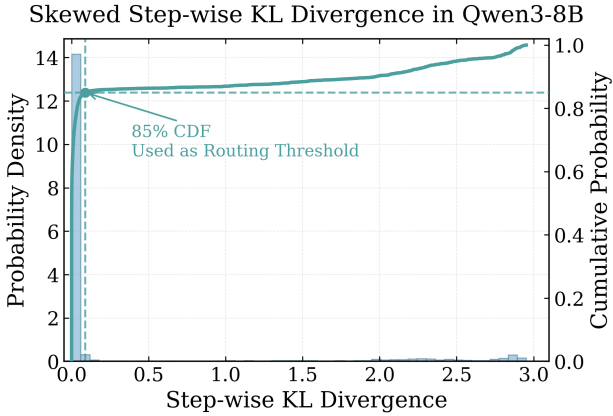


Figure 4. Distribution of step-wise KL divergence of 200 episodes between low-precision(3bit) and high-precision(bf16) policies of Qwen-8B on Alfworld. The distribution is highly skewed and bimodal-like: most decision steps exhibit near-zero divergence, while a small fraction forms a distant tail with substantially larger divergence values, with very few samples in between. In experiment, we choose 85% as the alpha of the model.

ment. This ensures that KL divergence is measured on near-golden trajectories rather than states induced by degraded low-precision rollouts. We further retain only trajectories that successfully complete the task objective and extract KL supervision signals exclusively from these trajectories.

Step-wise KL Divergence. Formally, for a given decision step t with state s_t , we define the step-wise behavioral divergence between the low-precision and high-precision models as

$$D_t = \text{KL}(\pi^{\text{low}}(\cdot | s_t) \parallel \pi^{\text{high}}(\cdot | s_t)), \quad (9)$$

where both action distributions are defined over the same action space. Each decision step is thus annotated with a KL value D_t together with its corresponding step-level state representation (X_t, m_t) .

KL-to-Classification Mapping. Due to the skewed nature of the KL distribution, directly regressing raw KL values is neither stable nor necessary for routing decisions. Instead, we transform D_t into a binary supervision signal that captures whether a step is likely to require high-precision inference. Specifically, we compute the empirical cumulative distribution function (CDF) of $\{D_t\}$ over the training set and assign

$$y_t = \begin{cases} 1, & \text{if } \text{CDF}(D_t) \geq \tau, \\ 0, & \text{otherwise,} \end{cases} \quad (10)$$

where $\tau \in (0, 1)$ is a fixed threshold. The positive class ($y_t = 1$) corresponds to steps that are predicted to require high-precision execution, while the negative class indicates that low-precision inference is sufficient.

KL-Supervised Fine-Tuning Objective. Let $\pi_\theta(r_t | s_t)$ denote the router policy defined in Section 4.1. We train the router via supervised training using the KL-derived classification labels. The optimization objective is given by

$$\mathcal{L}_{\text{KL-ST}}(\theta) = \mathbb{E}_{(X_t, y_t)} \left[-w_{y_t} \log \pi_\theta(r_t = y_t | s_t) \right], \quad (11)$$

where w_{y_t} denotes a class-specific weight inversely proportional to the empirical class frequency, mitigating the class imbalance induced by the heavy-tailed KL distribution.

This KL-ST stage provides a stable initialization for the router by distilling step-level behavioral discrepancies between low-precision and high-precision models, and serves as a warm start for subsequent reinforcement-based optimization.

4.3. GRPO Stage

Why GRPO for Routing. We adopt Group-Relative Policy Optimization (GRPO) to further refine the router after KL-ST initialization for two key reasons.

First, compared to PPO-style methods, GRPO does not rely on a learned value function. This property is particularly desirable in long-horizon agentic tasks with sparse rewards, where value estimation is often noisy. By using relative returns within a trajectory group, GRPO provides a low-variance advantage signal leading to more stable optimization.

Second, GRPO operates at the trajectory level and directly optimizes task-level outcomes, which is complementary to the step-level supervision provided by KL-ST. While KL-ST identifies precision-sensitive decision steps based on behavioral divergence, GRPO adjusts routing decisions based on their global impact on task success and inference cost. This orthogonality allows the router to benefit from both fine-grained step-level signals and end-to-end task-level optimization, hence consistently improved performance–cost trade-offs.

Group-Based Trajectory Sampling. Starting from the KL-ST initialized router, we sample groups of trajectories by interacting with the environment. For each task instance, we generate a group of K trajectories $\{\tau^{(1)}, \dots, \tau^{(K)}\}$ under the current router policy π_θ . Within each trajectory, the router selects the inference precision at every decision step, and the corresponding language model generates the action executed in the environment.

Each trajectory $\tau^{(i)}$ yields a task-level return $R(\tau^{(i)})$, which reflects task success and incorporate a penalty for high-precision usage, consistent with the objective defined in Equation (12).

5. Experiments

$$R(\tau^{(i)}) = \mathbb{I}[\tau^{(i)} \text{ succeeds}] - \mathcal{C}_{\text{High}}^{(i)} - \mathcal{C}_{\text{step}}^{(i)}. \quad (12)$$

The strong-inference cost $\mathcal{C}_{\text{strong}}^{(i)}$ captures the overhead of high-precision model usage and is defined as

$$\mathcal{C}_{\text{High}}^{(i)} = \lambda_{\text{High}} \cdot S^{(i)}, \quad (13)$$

where $S^{(i)}$ denotes the number of steps router selects the high-precision model, and λ_{High} specifies the cost per high-precision model invocation. While the step cost $\mathcal{C}_{\text{step}}^{(i)}$ penalizes long trajectories and is defined as

$$\mathcal{C}_{\text{step}}^{(i)} = \lambda_{\text{step}} \cdot T^{(i)}, \quad (14)$$

where $T^{(i)}$ denotes the number of total steps in trajectory $\tau^{(i)}$ and λ_{step} controls the per-step penalty..

Group-Relative Advantage. Rather than relying on an explicit value function, GRPO estimates an advantage signal by comparing trajectories within the same group. For a trajectory $\tau^{(i)}$, we define the group-relative advantage as

$$A^{(i)} = \frac{R(\tau^{(i)}) - \mu_R}{\sigma_R + \epsilon}, \quad (15)$$

where μ_R and σ_R denote the mean and standard deviation of returns within the same trajectory group, and ϵ is a small constant for numerical stability.

Router Policy Optimization. The router is optimized by maximizing the expected group-relative advantage via policy gradient. Specifically, the GRPO objective is given by

$$\begin{aligned} \mathcal{L}_{\text{GRPO}}(\theta) = & -\mathbb{E}_{\tau^{(i)}} \left[A^{(i)} \sum_t \log \pi_\theta \left(r_t^{(i)} \mid s_t^{(i)} \right) \right] \\ & + \beta \text{KL}(\pi_\theta \parallel \pi_{\theta_0}). \end{aligned} \quad (16)$$

where π_{θ_0} denotes the router policy obtained after the KL-ST stage and β controls the strength of the KL regularization. The KL term constrains policy updates to remain close to the supervised initialization, improving training stability.

This GRPO stage directly optimizes the router with respect to task reward and optimize at the task-level while KL-ST training on step-level signals. By combining KL-ST for stable start initialization and GRPO for end-task optimization, the router learns to selectively invoke high-precision inference at critical steps where it yields the greatest impact on overall task success.

5.1. Settings

ALFWorld. ALFWorld is a text-based embodied environment that aligns natural language instructions with household manipulation tasks. Each episode places the agent in a simulated indoor environment, where it must complete a high-level goal such as finding objects, interacting with containers, and operating appliances through a sequence of textual actions. At each step, the agent receives a textual observation describing the current environment state and outputs a natural-language action that is executed by the simulator.

ALFWorld tasks require planning ability under partial observability. Task success depends on maintaining coherent decision making over extended trajectories. These properties make ALFWorld a representative benchmark for evaluating agentic ability suitable for studying step-level routing strategies. For ALFWorld, we evaluate on the unseen test task following [Yao et al. \(2022b\)](#).

Metrics. We evaluate agent performance using both effectiveness and efficiency metrics. Following prior work, we report the *success rate*, defined as the fraction of evaluation episodes that successfully complete the task, and the *high-precision usage*, defined as the fraction of decision steps routed to the high-precision model.

To capture both task success and inference cost in a single metric, we introduce a unified efficiency measure termed *Gain per High-Precision Call (GHC)*. Let S denote the success rate of a given method, S_{weak} denote the success rate achieved by the low-precision model with 0% high-precision calls, and $c \in (0, 1]$ denote the high-precision ratio. We define

$$\text{GHC} = \frac{S - S_{\text{weak}}}{c}.$$

GHC measures how effectively each unit of high-precision model budget translates into improvements in task success. When $c = 0$, GHC is undefined and therefore omitted, as no high-precision calls are used. A higher GHC indicates a better tradeoff between overall system efficiency and performance gain, as illustrated in Fig. 5 as The slope relative to the low-precision model.

In all results, we report success rate and high-precision usage alongside GHC to provide a complete view of the performance-cost trade-off.

Experimental Models and Precision. We evaluate our method on two representative open-source model families with different training stages. Specifically, **Qwen** models are used in their *post-training* form released by the authors, reflecting instruction-tuned and aligned models commonly

Table 1. Routing Performance. Gain per High-Precision Call (GHC) measures the slope of tradeoff between efficiency and success rate gain compared to quantized only inference. A higher GHC indicates a better tradeoff, as illustrated in Fig. 5.

Model	Method	High-Precision Ratio	Success Rate	GHC ↑
Qwen3-8B	BF16	100%	89.6%	6.8
	GPTQ-3Bit	0%	82.8%	–
	Random@20%	20%	83.2%	2
	Random@40%	40%	86.2%	8.5
	Random@60%	60%	84.83%	3.38
	Random@80%	80%	87.7%	6.13
	Router(Ours)	26.7%	88.8%	19.85
	BF16	100%	93.3%	15.7
Qwen3-4B	GPTQ-3Bit	0%	77.6%	–
	Random@20%	20%	78.1%	2.5
	Random@40%	40%	81.1%	8.75
	Random@60%	60%	88.8%	18.67
	Random@80%	80%	90.3%	15.88
	Router(Ours)	8.6%	81.3%	43.02
	BF16	100%	69.4%	14.9
	GPTQ-Int4	0%	54.5%	–
Qwen3-1.7B	Random@20%	20%	56.2%	8.5
	Random@40%	40%	60.5%	15
	Random@60%	60%	61.9%	12.33
	Random@80%	80%	65.7%	14
	Router(Ours)	20.5%	59%	21.95
	BF16	100%	62.7%	18.7
	GPTQ-Int4	0%	44%	–
	Random@20%	20%	45.3%	6.5
DeepSeek-R1-Distill-Llama-8B	Random@40%	40%	48.1%	10.25
	Random@60%	60%	51.6%	12.67
	Random@80%	80%	54.2%	12.75
	Router(Ours)	9.8%	47.8%	38.77

deployed in practice. Besides, we include **DeepSeek-R1-Distill** models, which are obtained by distilling strong reasoning models into smaller backbones, representing a distilled reasoning model family.

Across these families, we conduct experiments on models of different scales, including Qwen3-8B/4B/1.7B, as well as DeepSeek-R1-Distill-Llama3-8B. For efficiency baselines, we construct low-precision variants using **GPTQ** quantization with **3-bit** and **4-bit**weights. For Qwen3-4B and Qwen3-8B, we use 3-bit GPTQ quantization, while for Qwen1.7B and DeepSeek-R1-Distill-Llama3-8B, we adopt 4-bit GPTQ quantization.

5.2. Results

Overall Performance. Table 1 shows that our router consistently achieves a superior accuracy–cost trade-off across model scales. Compared to random routing under matched high-precision model budgets, our method yields higher success rates with significantly fewer high-precision calls. Notably, our method often approaches the performance of full-precision BF16 models while using less than 30% of high-precision steps.

Efficiency Analysis. We further analyze efficiency using GHC. The router achieves the highest GHC across all evaluated settings, indicating that each high-precision model invocation contributes more effectively to task success com-

pared to heuristic baselines.

5.3. Ablation Study

We conduct ablation studies to analyze the roles of the two core components in our routing framework: (i) KL-divergence–guided supervision (KL-ST) for training data construction, and (ii) Cost-aware GRPO policy optimization for improving routing decisions. All ablations are evaluated on the same benchmark and follow the same evaluation protocol as the main results.

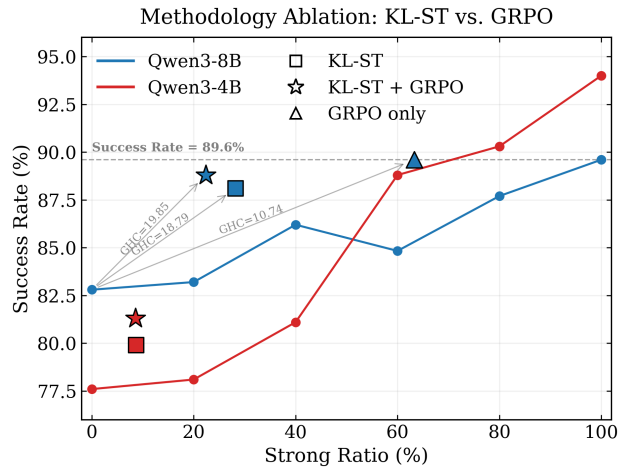


Figure 5. Methodology ablation comparing KL-ST and KL-ST + GRPO routing on Qwen3-8B and Qwen3-4B; GRPO-only is evaluated on Qwen3-8B. Success rate is plotted against high-precision usage ratio. Solid curves show the baseline trade-off frontiers for Qwen3-8B (blue) and Qwen3-4B (red) with random routing, while markers denote different routing strategies. The GHC metric is visualized as the slope of the line connecting the low-precision model to each method.

Effect of GRPO Training. We examine the effect of GRPO by comparing three variants: *KL-ST only*, where the router is trained with KL-divergence–guided supervision without policy optimization; *GRPO-only*, which applies policy optimization from scratch; and the full model (*KL-ST + GRPO*), which combines both components by applying GRPO on top of the KL-ST-trained weights.

As shown in Figure 5, incorporating GRPO improves routing performance over KL-ST-only training on both Qwen3-4B and Qwen3-8B. This improvement indicates that policy optimization enables the router to allocate high-precision model calls more effectively by explicitly penalizing high-precision model usage in the GRPO objective. In contrast to KL-ST, which relies on KL-divergence–based supervision, GRPO directly optimizes task-level rewards, leading to higher success rates.

Table 2. Ablation of GRPO on top of KL-ST routing on ALFWorld.

Model	Variant	HR \downarrow	Succ. \uparrow	GHC \uparrow
Qwen3-8B	KL-ST	28.2	88.1	18.79
	GRPO	63.3	89.6	10.74
	KL-ST + GRPO	26.7	88.8	19.85
Qwen3-4B	KL-ST	8.7	79.9	26.43
	KL-ST + GRPO	8.6	81.3	43.02
Qwen3-1.7B	KL-ST	20.5	59	21.95
	KL-ST + GRPO	20.5	59	21.95
DeepSeek-R1- Distill-Llama-8B	KL-ST	9.8	47	30.61
DeepSeek-R1- Distill-Llama-8B	KL-ST + GRPO	9.8	47.8	38.77

GRPO-only training achieves a success rate (89.6%) comparable to the high-precision model while using only 63.3% high-precision model calls, demonstrating the effectiveness for reducing high-precision model usage. However, compared to methods incorporating KL-ST, GRPO-only is less efficient, as KL-ST improves both the precision and recall of the binary routing classifier during training, leading to a more favorable performance–cost trade-off.

From Table 2, We further observe that the performance gains brought by GRPO are correlated with the capability of the underlying high-precision model (**HR** denotes the high-precision rate). The largest improvement in GHC is achieved on Qwen3-4B, which also exhibits the highest success rate among the evaluated models, while no additional gains are observed on the smallest backbone, Qwen3-1.7B.

We attribute this behavior to the inherent limitation of the router’s action space. The router can only influence performance by selecting which action model to query, but cannot directly generate actions or modify the internal parameters of the action models. As a result, the effectiveness of routing-based optimization is bounded by the expressiveness and capability of the high-precision model itself. When the high-precision model is sufficiently capable, improved routing decisions can better exploit its strengths and yield meaningful performance gains. In contrast, when the high-precision model is weak, routing alone offers limited room for improvement, leading to diminishing returns from policy optimization.

Effect of KL-ST Data Scale. We further study how the amount of KL-ST training data affects routing performance. Specifically, we vary the number of episodes used to construct KL-divergence-based supervision while keeping the router architecture and training procedure fixed.

As shown in Table 3, increasing the number of KL-ST episodes generally leads to improvements in the GHC metric, indicating that richer KL-based supervision provide the router with a clearer decision boundary. Although GHC

Table 3. Ablation on the training data scale of KL-ST.

KL-ST Episodes	SR(%) \downarrow	Succ.(%) \uparrow	GHC \uparrow
100	20.4	85.8	14.71
200	28.2	88.1	18.79
300	10.3	84.3	14.56
400	9.1	85.1	25.27

improves from 100 to 200 episodes although 300 episodes exhibiting fluctuations.

Figure 6 provides a geometric interpretation of this trend by plotting success rate against high-precision model usage. Models trained by KL-ST consistently lies above the best baseline, the black dashed diagonal line denotes the best-performing baseline.

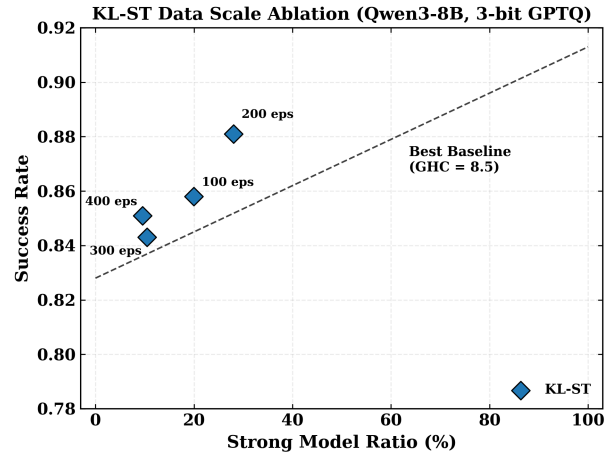


Figure 6. Success rate versus high-precision usage for KL-ST trained with different supervision scales. The dashed line indicates the best baseline gain-per-high-precision-call (GHC = 8.5), and increasing KL-ST supervision generally improves performance–cost efficiency.

6. Conclusion

In this paper, we study multi-steps LLM interaction in agentic setting through dynamic precision routing. We show that sensitivity to numerical precision is highly uneven across decision steps, and that invoking high-precision models only at a small number of critical steps is sufficient to achieve strong task performance. Based on this observation, we propose a lightweight step-level mix-precision router trained with KL-divergence-guided supervision and cost-aware policy optimization. Experiments across multiple models and precisions demonstrate that our method consistently achieves superior performance–cost trade-offs.

References

Chen, L., Zaharia, M., and Zou, J. Frugalgpt: How to use large language models while reducing cost and improving performance. *Trans. Mach. Learn. Res.*, 2024, 2024a. URL <https://openreview.net/forum?id=cSimKw5p6R>.

Chen, S., Jiang, W., Lin, B., Kwok, J. T., and Zhang, Y. Routerdc: Query-based router by dual contrastive learning for assembling large language models. In Globersons, A., Mackey, L., Belgrave, D., Fan, A., Paquet, U., Tomczak, J. M., and Zhang, C. (eds.), *Advances in Neural Information Processing Systems 38: Annual Conference on Neural Information Processing Systems 2024, NeurIPS 2024, Vancouver, BC, Canada, December 10 - 15, 2024*, 2024b.

Dettmers, T., Lewis, M., Belkada, Y., and Zettlemoyer, L. Gpt3.int8(): 8-bit matrix multiplication for transformers at scale. In Koyejo, S., Mohamed, S., Agarwal, A., Belgrave, D., Cho, K., and Oh, A. (eds.), *Advances in Neural Information Processing Systems 35: Annual Conference on Neural Information Processing Systems 2022, NeurIPS 2022, New Orleans, LA, USA, November 28 - December 9, 2022*, 2022.

Ding, D., Mallick, A., Wang, C., Sim, R., Mukherjee, S., Rühle, V., Lakshmanan, L. V. S., and Awadallah, A. H. Hybrid LLM: cost-efficient and quality-aware query routing. In *The Twelfth International Conference on Learning Representations, ICLR 2024, Vienna, Austria, May 7-11, 2024*. OpenReview.net, 2024. URL <https://openreview.net/forum?id=02f3mUtqnM>.

Ding, D., Mallick, A., Zhang, S., Wang, C., Madrigal, D., del Carmen Hipolito Garcia, M., Xia, M., Lakshmanan, L. V. S., Wu, Q., and Rühle, V. Best-route: Adaptive LLM routing with test-time optimal compute. In *Forty-second International Conference on Machine Learning, ICML 2025, Vancouver, BC, Canada, July 13-19, 2025*. OpenReview.net, 2025. URL <https://openreview.net/forum?id=tFBIbCVXkG>.

Dong, P., Tang, Z., Liu, X., Li, L., Chu, X., and Li, B. Can compressed llms truly act? an empirical evaluation of agentic capabilities in LLM compression. In *Forty-second International Conference on Machine Learning, ICML 2025, Vancouver, BC, Canada, July 13-19, 2025*. OpenReview.net, 2025. URL <https://openreview.net/forum?id=rkwXYSDKso>.

Jiang, D., Ren, X., and Lin, B. Y. Llm-blender: Ensembling large language models with pairwise ranking and generative fusion. In Rogers, A., Boyd-Graber, J. L., and Okazaki, N. (eds.), *Proceedings of the 61st Annual Meeting of the Association for Computational Linguistics (Volume 1: Long Papers), ACL 2023, Toronto, Canada, July 9-14, 2023*, pp. 14165–14178. Association for Computational Linguistics, 2023. doi: 10.18653/v1/2023.ACL-LONG.792. URL <https://doi.org/10.18653/v1/2023.acl-long.792>.

Jimenez, C. E., Yang, J., Wettig, A., Yao, S., Pei, K., Press, O., and Narasimhan, K. R. Swe-bench: Can language models resolve real-world github issues? In *The Twelfth International Conference on Learning Representations, ICLR 2024, Vienna, Austria, May 7-11, 2024*. OpenReview.net, 2024. URL <https://openreview.net/forum?id=VTF8yNQM66>.

Jin, R., Du, J., Huang, W., Liu, W., Luan, J., Wang, B., and Xiong, D. A comprehensive evaluation of quantization strategies for large language models. In Ku, L.-W., Martins, A., and Srikumar, V. (eds.), *Findings of the Association for Computational Linguistics: ACL 2024*, pp. 12186–12215, Bangkok, Thailand, August 2024. Association for Computational Linguistics. doi: 10.18653/v1/2024.findings-acl.726. URL <https://aclanthology.org/2024.findings-acl.726>.

Jitkrittum, W., Narasimhan, H., Rawat, A. S., Juneja, J., Wang, Z., Lee, C., Shenoy, P., Panigrahy, R., Menon, A. K., and Kumar, S. Universal model routing for efficient LLM inference. *CoRR*, abs/2502.08773, 2025. doi: 10.48550/ARXIV.2502.08773. URL <https://doi.org/10.48550/arXiv.2502.08773>.

Li, X., Jiao, W., Jin, J., Dong, G., Jin, J., Wang, Y., Wang, H., Zhu, Y., Wen, J., Lu, Y., and Dou, Z. Deepagent: A general reasoning agent with scalable toolsets. *CoRR*, abs/2510.21618, 2025a. doi: 10.48550/ARXIV.2510.21618. URL <https://doi.org/10.48550/arXiv.2510.21618>.

Li, Z., Su, Y., Yang, R., Xie, C., Wang, Z., Xie, Z., Wong, N., and Yang, H. Quantization meets reasoning: Exploring llm low-bit quantization degradation for mathematical reasoning, 2025b. URL <https://arxiv.org/abs/2501.03035>.

Lin, J., Tang, J., Tang, H., Yang, S., Chen, W., Wang, W., Xiao, G., Dang, X., Gan, C., and Han, S. AWQ: activation-aware weight quantization for on-device LLM compression and acceleration. In Gibbons, P. B., Pekhimenko, G., and Sa, C. D. (eds.), *Proceedings of the Seventh Annual Conference on Machine Learning and Systems, MLSys 2024, Santa Clara, CA, USA, May 13-16, 2024*. mlsys.org, 2024.

Liu, R., Sun, Y., Zhang, M., Bai, H., Yu, X., Yu, T., Yuan, C., and Hou, L. Quantization hurts reason-

ing? an empirical study on quantized reasoning models. *CoRR*, abs/2504.04823, 2025. doi: 10.48550/ARXIV.2504.04823. URL <https://doi.org/10.48550/arXiv.2504.04823>.

Ong, I., Almahairi, A., Wu, V., Chiang, W.-L., Wu, T., Gonzalez, J., Kadous, M. W., and Stoica, I. Routellm: Learning to route llms from preference data. In *International Conference on Learning Representations*, 2025a. URL <https://api.semanticscholar.org/CorpusID:278498837>.

Ong, I., Almahairi, A., Wu, V., Chiang, W.-L., Wu, T., Gonzalez, J. E., Kadous, M. W., and Stoica, I. Routellm: Learning to route llms with preference data, 2025b. URL <https://arxiv.org/abs/2406.18665>.

Qiao, Z., Chen, G., Chen, X., Yu, D., Yin, W., Wang, X., Zhang, Z., Li, B., Yin, H., Li, K., Min, R., Liao, M., Jiang, Y., Xie, P., Huang, F., and Zhou, J. Webresearcher: Unleashing unbounded reasoning capability in long-horizon agents. *CoRR*, abs/2509.13309, 2025. doi: 10.48550/ARXIV.2509.13309. URL <https://doi.org/10.48550/arXiv.2509.13309>.

Schick, T., Dwivedi-Yu, J., Dessì, R., Raileanu, R., Lomeli, M., Hambro, E., Zettlemoyer, L., Cancedda, N., and Scialom, T. Toolformer: Language models can teach themselves to use tools. *Advances in Neural Information Processing Systems*, 36:68539–68551, 2023.

Shazeer, N., Mirhoseini, A., Maziarz, K., Davis, A., Le, Q. V., Hinton, G. E., and Dean, J. Outrageously large neural networks: The sparsely-gated mixture-of-experts layer. In *5th International Conference on Learning Representations, ICLR 2017, Toulon, France, April 24-26, 2017, Conference Track Proceedings*. OpenReview.net, 2017. URL <https://openreview.net/forum?id=B1ckMDqlg>.

Shinn, N., Cassano, F., Gopinath, A., Narasimhan, K., and Yao, S. Reflexion: Language agents with verbal reinforcement learning. *Advances in Neural Information Processing Systems*, 36:8634–8652, 2023.

Shridhar, M., Yuan, X., Côté, M., Bisk, Y., Trischler, A., and Hausknecht, M. J. Alfworld: Aligning text and embodied environments for interactive learning. In *9th International Conference on Learning Representations, ICLR 2021, Virtual Event, Austria, May 3-7, 2021*. OpenReview.net, 2021. URL <https://openreview.net/forum?id=0IOX0YcCdTn>.

Si, W., Jang, S., Lee, I., and Bastani, O. Conformal constrained policy optimization for cost-effective llm agents, 2025. URL <https://arxiv.org/abs/2511.11828>.

Wang, G., Xie, Y., Jiang, Y., Mandlekar, A., Xiao, C., Zhu, Y., Fan, L., and Anandkumar, A. Voyager: An open-ended embodied agent with large language models. *Trans. Mach. Learn. Res.*, 2024, 2024a. URL <https://openreview.net/forum?id=ehfRiF0R3a>.

Wang, N., Hu, X., Liu, P., Zhu, H., Hou, Y., Huang, H., Zhang, S., Yang, J., Liu, J., Zhang, G., Zhang, C., Wang, J., Jiang, Y. E., and Zhou, W. Efficient agents: Building effective agents while reducing cost, 2025. URL <https://arxiv.org/abs/2508.02694>.

Wang, R., Jansen, P. A., Côté, M., and Ammanabrolu, P. Scienceworld: Is your agent smarter than a 5th grader? In Goldberg, Y., Kozareva, Z., and Zhang, Y. (eds.), *Proceedings of the 2022 Conference on Empirical Methods in Natural Language Processing, EMNLP 2022, Abu Dhabi, United Arab Emirates, December 7-11, 2022*, pp. 11279–11298. Association for Computational Linguistics, 2022. doi: 10.18653/V1/2022.EMNLP-MAIN.775. URL <https://doi.org/10.18653/v1/2022.emnlp-main.775>.

Wang, X., Chen, Y., Yuan, L., Zhang, Y., Li, Y., Peng, H., and Ji, H. Executable code actions elicit better LLM agents. In *Forty-first International Conference on Machine Learning, ICML 2024, Vienna, Austria, July 21-27, 2024*. OpenReview.net, 2024b. URL <https://openreview.net/forum?id=jJ9BoXAfFa>.

Wu, D., Wang, J., Meng, Y., Zhang, Y., Sun, L., and Wang, Z. CATP-LLM: empowering large language models for cost-aware tool planning. *CoRR*, abs/2411.16313, 2024. doi: 10.48550/ARXIV.2411.16313. URL <https://doi.org/10.48550/arXiv.2411.16313>.

Xiong, N., Zhou, Y., Zeng, H., Chen, Z., Huang, F., Bi, S., Zhang, L., and Zhao, Z. Token-level llm collaboration via fusionroute, 2026. URL <https://arxiv.org/abs/2601.05106>.

Yang, J., Jimenez, C. E., Wettig, A., Lieret, K., Yao, S., Narasimhan, K., and Press, O. Swe-agent: Agent-computer interfaces enable automated software engineering. In Globersons, A., Mackey, L., Belgrave, D., Fan, A., Paquet, U., Tomczak, J. M., and Zhang, C. (eds.), *Advances in Neural Information Processing Systems 38: Annual Conference on Neural Information Processing Systems 2024, NeurIPS 2024, Vancouver, BC, Canada, December 10 - 15, 2024*, 2024.

Yao, S., Chen, H., Yang, J., and Narasimhan, K. Webshop: Towards scalable real-world web interaction with grounded language agents. In Koyejo, S., Mohamed, S., Agarwal, A., Belgrave, D., Cho, K., and Oh, A. (eds.), *Advances in Neural Information Processing Systems 35: Annual Conference on Neural Information Processing*

*Systems 2022, NeurIPS 2022, New Orleans, LA, USA,
November 28 - December 9, 2022a.*

Yao, S., Zhao, J., Yu, D., Du, N., Shafran, I., Narasimhan, K. R., and Cao, Y. React: Synergizing reasoning and acting in language models. In *The eleventh international conference on learning representations*, 2022b.

Yue, Y., Zhang, G., Liu, B., Wan, G., Wang, K., Cheng, D., and Qi, Y. MasRouter: Learning to route LLMs for multi-agent systems. In Che, W., Nabende, J., Shutova, E., and Pilehvar, M. T. (eds.), *Proceedings of the 63rd Annual Meeting of the Association for Computational Linguistics (Volume 1: Long Papers)*, pp. 15549–15572, Vienna, Austria, July 2025. Association for Computational Linguistics. ISBN 979-8-89176-251-0. doi: 10.18653/v1/2025.acl-long.757. URL <https://aclanthology.org/2025.acl-long.757/>.

Zhang, H., Feng, T., and You, J. Router-r1: Teaching llms multi-round routing and aggregation via reinforcement learning. *CoRR*, abs/2506.09033, 2025. doi: 10.48550/ARXIV.2506.09033. URL <https://doi.org/10.48550/arXiv.2506.09033>.

Zhou, S., Xu, F. F., Zhu, H., Zhou, X., Lo, R., Sridhar, A., Cheng, X., Ou, T., Bisk, Y., Fried, D., Alon, U., and Neubig, G. Webarena: A realistic web environment for building autonomous agents. In *The Twelfth International Conference on Learning Representations, ICLR 2024, Vienna, Austria, May 7-11, 2024*. OpenReview.net, 2024. URL <https://openreview.net/forum?id=oKn9c6ytLx>.

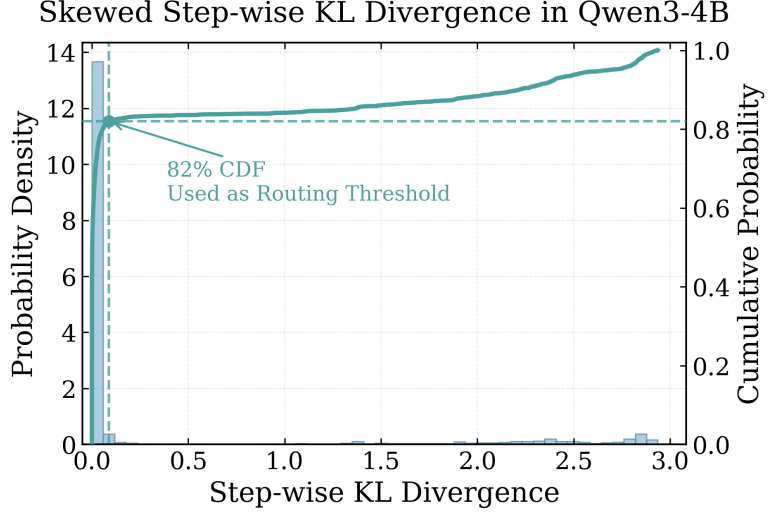


Figure 7. Distribution of step-wise KL divergence for an Qwen3-4B. The distribution exhibits a similar heavy-tailed pattern as observed in the main text, suggesting that the phenomenon generalizes across model variants.

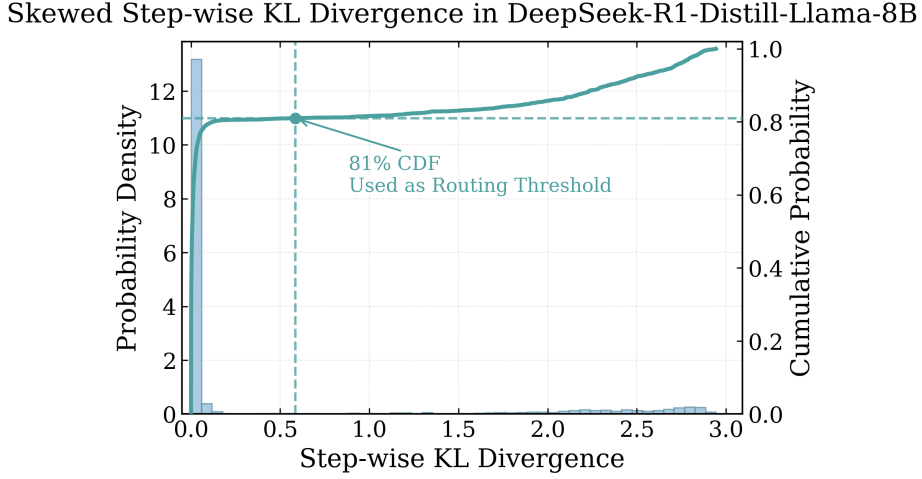


Figure 8. Distribution of step-wise KL divergence for DeepSeek-R1-Distill-Llama-8B.

A. Additional Experimental Details.

A.1. KL Divergence Distributions Across Models

Figure 7 and 8 shows the distribution of step-wise KL divergence for Qwen3-4B. We observe a similarly skewed distribution with a long right tail, indicating that precision-critical steps are concentrated in a small fraction of the trajectory rather than being uniformly distributed.

A.2. Case Study: A Trajectory Where Routing Succeeds but Low-Precision Fails

To provide qualitative insights into the effectiveness of our routing strategy, we present a representative interaction trajectory in which the router successfully completes the task while the low-precision model fails. Although both models follow similar high-level plans, the low-precision model fails to correctly handle a critical state-transition step, leading to an incorrect task outcome. In contrast, the router selectively invokes the high-precision at this critical step, ensuring a correct state update and successful task completion.

Task A: Clean Cloth and Store. **Task Description.** You are in the middle of a room. Your task is to clean a piece of cloth and put it into a cabinet.

Low-Precision Model Trajectory (Failure).

- **Object acquisition.** The agent locates a handtowel from a towel holder and picks it up.
- **Critical step: cleaning.**
 - Action: clean handtowel with sinkbasin
 - Observation: *Nothing happens.*

The agent repeatedly retries the cleaning action but fails to recognize that the cloth remains unclean.

- **Incorrect state assessment.** Despite the failed cleaning attempts, the agent assumes the cloth is clean.
- **Premature termination.**
 - Action: move handtowel to cabinet

Outcome. The task fails because the cloth is stored without being successfully cleaned.

Router Trajectory (Success).

- **High-level planning (strong).** The router reasons about likely locations of the cloth and determines an efficient exploration strategy.
- **Exploration (cheap).** The agent checks sinkbasins and garbageman using the low-precision model.
- **Visual inspection (strong).**
 - Action: go to countertop 1
- **Cabinet search (cheap).** The agent opens multiple cabinets until the cloth is found.
- **Object acquisition (strong).**
 - Action: take cloth 1 from cabinet 4
- **Navigation to sinkbasin (strong).**
 - Action: go to sinkbasin 1
- **Cleaning (cheap).**
 - Action: clean cloth 1 with sinkbasin 1
 - Observation: *The cloth is successfully cleaned.*
- **Task completion (cheap).**
 - Action: move cloth 1 to cabinet 1

B. Training Details

Router Training with KL-ST. The binary router is trained using KL-ST supervision constructed from 200 episodes. We optimize the router for 5 epochs with a batch size of 64 and a learning rate of 1×10^{-4} . Model selection is performed by choosing the checkpoint that achieves the highest validation accuracy across all training epochs. Unless otherwise specified, the routing threshold is manually selected based on the empirical distribution of step-wise KL divergence and lies between the 78th and 85th percentiles.

GRPO-based Reinforcement Learning. Following KL-ST pretraining, we further refine the router using Group-Relative Policy Optimization (GRPO). For each task instance, the router samples K rollouts to estimate trajectory-level returns. The GRPO training budget consists of 120 episodes in total. We set the high-precision model invocation cost to $\text{STRONG_COST} = 0.02$, the learning rate to 1×10^{-6} , and the KL regularization coefficient to $\beta_{\text{KL}} = 0.02$. For the GRPO-only ablation study, we keep the episode budget identical to the main GRPO setting and train the router using 320 episodes in total.